



Seismic fragility analysis of a three-story cross-laminated timber building considering near and far field ground motions

Saeid Javidi¹ · Igor Gavric² · Georgios Fourlaris¹ · Mohammad Reza Salami³

Received: 23 October 2024 / Accepted: 18 June 2025
© The Author(s) 2025

Abstract

This paper investigates the seismic response of the three-story Cross-Laminated Timber (CLT) building of the SOFIE project subjected to the Near-Field (NF) Far-Field (FF) ground motions according to FEMA P-695. The numerical models have been developed in connector, wall and full-scale building levels in OpenSees. Nonlinear nonlinear springs have been utilised to model the behaviour of CLT connectors while considering Gap joints only to transfer compression forces between panels and the rigid foundation without the ability to carry tensile forces. The CLT panels have been modelled as moment-resisting frames by applying elastic beam elements with high stiffness. The panel-to-panel and panel-to-foundation friction has also been considered by modifying the initial stiffness of the CLT connector springs. The building was analysed using Incremental Dynamic Analysis (IDA), including 2450 time-history simulations, to assess its behaviour during ground motions. Significant Damage (SD) and Near-Collapse (NC) damage stated have been identified for the building based on EN12512 standard through Modal Push-over Analysis (MPA). Subsequently, the fragility curves have been developed for the CLT building under NF and FF ground motions. The IDA curves prove that the CLT building considered in this paper is more affected by Near-Field Pulse-like (NF-P) than by Near-Field No-Pulse (NF-NP) and FF ground motions. Moreover, the modelled building is significantly more affected by NF-P ground motions than by NF-NP and FF motions, with a higher probability of collapse under NF-P conditions.

Keywords Cross-laminated timber · Incremental dynamic analysis · Fragility analysis · Near-field and Far-Field ground motions

✉ Saeid Javidi
saeid.javidi@bcu.ac.uk

¹ College of Built Environment, Birmingham City University, Birmingham B5 5JU, UK

² Mass Timber Structural Engineer, Element5 Limited Partnership, Toronto, CA, Canada

³ School of Engineering, University of Birmingham, Birmingham B15 2TT, UK

1 Introduction

The evolution of engineered wood technologies, notably Cross-Laminated Timber (CLT) and Glued-Laminated Timber (GLT) marks a significant shift towards more sustainable and earthquake-resilient construction methods of timber buildings. These improvements take advantage of wood's natural benefits, such as an exceptional strength-to-weight ratio and reduced carbon dioxide emissions and present an environmentally friendly alternative to traditional construction materials such as steel and concrete. Despite these advantages, the application of wood in taller structures has faced challenges, including limitations in size, the presence of natural defects, design challenges, especially for resisting lateral forces from wind and earthquakes (Tannert and Loss 2022). Engineered Wood Products (EWPs) address these limitations by offering improved structural capabilities and paving the way for the utilisation of wood in more ambitious architectural designs. According to Green and Taggart (2020), EWPs have successfully mitigated the traditional constraints of wood and facilitated its application in larger-scale constructions.

The seismic resilience of timber constructions has been increasingly discussed, with a significant shift towards the utilization of timber in the development of medium to high-rise buildings. This transition is attributed to timber's sustainable, resilient, and renewable properties. Despite being a relatively new option, CLT buildings have quickly gained popularity in the European market, which has traditionally favoured structural solutions using masonry or concrete over lighter materials like timber. Because of the layers crossing each other, CLT panels are suitable for use as flat components like walls and floors. The key benefit is the quick assembly, as all panels are made off-site, cut to fit, transported to the construction site, and easily joined together using metal connectors like hold-downs, angle brackets, and screws.

Several researchers have conducted experiments and computational analyses on CLT assemblies and full-scale building models to evaluate their performance under various static and dynamic loads. Ceccotti et al. (2006); Ceccotti et al. (2013) conducted multiple studies under the SOFIE project on the structural behaviour and seismic design of timber buildings. Their studies have significantly contributed to the CLT structures' response to seismic forces and design practices in seismic zones. Dujic et al. (2010) evaluated the seismic performance of the three-story CLT building of the SOFIE project. They developed numerical models to assess the dynamic behaviour of timber buildings during earthquakes. Additionally, Popovski et al. (2014) conducted quasi-static tests on a two-story full-scale CLT building to evaluate the building's global response and the shear wall's performance. Rinaldin and Fragiaco (2016) developed an advanced FE model to simulate the seismic response of CLT buildings as part of the SOFIE project. This model was used to reproduce experimental results from shaking table tests carried out on three- and seven-story full-scale CLT buildings in Japan. The model, characterized by its capacity to incorporate non-linear dynamic analyses and detailed descriptions of metal connectors, effectively captured the seismic responses with high accuracy, demonstrating less than 20% error in relative acceleration and less than 7% in roof displacement. Moreover, Latour and Rizzano (2017) studied the seismic design of mixed CLT and light-frame shear wall buildings. They proposed an analytical formulation for estimating the behaviour factor for the mixed system to improve the application of EC 8's force-based design philosophy. In other studies, Pozza, Ferracuti, et al. (2018); Pozza, Saetta, et al. (2018) and Pozza, Savoia, et al. (2018) investigated the cyclic

behaviour of CLT-wall systems for seismic applications. They compared phenomenological and component-level modelling approaches to understand the behaviour of the CLT panel-connection system globally and locally. Additionally, several investigations have been conducted to study the seismic parameters of hybrid buildings' fragility assessment of CLT walls and buildings such as Tesfamariam et al. (2014), Bezabeh et al. (2016), Bezabeh et al. (2018), Kovacs and Wiebe (2019), Shahnewaz et al. (2020), Roncari et al. (2020), Aloisio et al. (2021), Aloisio et al. (2022), Pan et al. (2023), Zhang and Loss (2023), Teweldebrhan et al. (2023) and Ho et al. (2024). These studies collectively offer a perspective on the fragility of hybrid buildings, where CLT systems and various structural elements are combined.

Following these extensive experimental and analytical studies on CLT seismic performance, recent research has focused on improving the seismic strength of timber buildings through new design methods and updates to building codes. Stepinac et al. (2020) discussed the seismic resilience of timber constructions by presenting a shift towards the utilisation of timber in the development of medium to high-rise buildings. This transition is attributed to timber's sustainable, resilient, and renewable properties. Despite being a relatively new option, CLT buildings have quickly gained popularity in the European market, which has traditionally favoured structural solutions using masonry or concrete over lighter materials like timber (Latour and Rizzano 2017). Because of the layers crossing each other, these panels are suitable for use as flat components like walls and floors. The key benefit is the quick assembly, as all panels are made off-site, cut to fit, transported to the construction site, and easily joined together using metal connectors like hold-downs, angle brackets and screws (Rinaldin and Fragiaco 2016). Follesa and Fragiaco (2018) investigated the seismic behaviour of mixed multi-story wood buildings combining CLT and Light-Frame shear walls which led to the identification of a gap in Eurocode 8 (EC 8) regarding guidance for buildings that utilise multiple lateral load-resisting systems at the same level (Code 2005). They suggest an analytical method for estimating the q -factor of mixed systems by applying the force-based philosophy of EC 8 in the seismic design of the studied buildings. In another study, Vassallo et al. (2018) detailed the design and construction of a six-story residential CLT building in Italy. They applied a proposed revision to EC 8 and examined its practicality for seismic design. Their research focused on the seismic design of CLT buildings and the importance of hold-down to foundation connection as a pivotal component in structures' resilience. Furthermore, Rinaldi et al. (2023) evaluated the proposed q -values against the seismic performance of CLT buildings designed according to the second generation of EC8 standard utilizing parametric non-linear static analyses and a risk-consistent methodology involving Incremental Dynamic Analyses (IDA) and fragility curves. The research concluded that the q -factors of 2.30 for ductility class 2 (DC2) and 3.20 for ductility class 3 (DC3) are reasonably acceptable. The structures' earthquake vulnerability can be assessed by conducting IDA and developing fragility curves to estimate potential damage at different performance levels. For this purpose, the structural performance levels could be determined through probabilistic assessment.

Despite their growing popularity, the current Eurocode 8 lacks specific provisions for CLT structures. As a result, existing seismic design rules do not fully incorporate recent advancements in the understanding of timber structures under seismic loading, particularly the introduction of different ductility classes and newly calibrated behaviour factors (q -factors) that reflect the unique properties of CLT panels (Rinaldi et al. 2023). This gap underscores the need for detailed investigations to ensure the structural safety of CLT build-

ings across varying seismic intensities. This study addresses that need by introducing a new numerical modelling approach tailored to simulate the full-scale seismic behaviour of CLT buildings subjected to Near-Field (NF) and Far-Field (FF) ground motions, following FEMA P-695 guidelines (FEMA 2009). Unlike previous studies, which often focus solely on simplified or component-level analysis, the novelty of this research lies in the development and validation of a comprehensive finite element (FE) model that integrates behaviour from the connector level to the full building scale. This model allows for efficient and accurate time-history simulations. By applying IDA, fragility curves are generated to quantify damage probability under seismic loading. The key contribution of this work is its methodological framework, which enables a more complete performance-based seismic assessment of CLT buildings.

2 Modelling

The numerical modelling approach is based on the capacity-based design principles which centralized the displacements in energy-dissipative connectors and rely on the stiff linear behaviour of the CLT panels. Therefore, connectors are responsible for ductility and energy dissipation in the building (Casagrande et al. 2019; Christovasilis et al. 2020; Gavric and Popovski 2014). Subsequently, the numerical model has been developed for the connector, wall, and building levels in OpenSees (McKenna 2011) to investigate its seismic response under various ground motions with different characteristics at the building level.

2.1 Connector level

A comprehensive experimental study was conducted in 2015 to analyse the behaviour of various types of connectors used in the three-story CLT building of the SOFIE project by (Gavric et al. 2015c). Angle brackets and hold-downs were employed for the wall panel-to-floor panel connections and for connecting the ground-floor wall panels to the foundation. Two types of connections used for wall panel to foundation and wall panel to floor panel connection in the three-story CLT building were tested. The WHT540 type hold-down with twelve 4×60 mm Anker annular ring nails have been used for the wall panel to foundation connection while anchored to the base using 16 mm bolts. WHT440 hold-downs have been nailed for wall-panel-to-floor panel connections using nine nails of the same type as those used in the wall-to-foundation connections. For the angle brackets in the foundation connection, BMF $90 \times 116 \times 48 \times 3$ mm brackets were employed, secured with eleven 4×60 mm Anker annular ring nails. These brackets were anchored to the foundations with a U12 bolt, similar to those used at the ground level of the three-story SOFIE building. In the panel-to-panel connections, the brackets used were BMF $100 \times 100 \times 90 \times 3$ mm, representing the wall-floor connection in the upper stories of the three-story CLT building. These brackets were attached to the wall panel with eight 4×60 mm annular ring nails and to the floor with six 4×60 mm annular ring nails, supplemented by two additional HBS 4×60 mm screws. Additionally, (Gavric et al. 2015b) tested all different types of panel-to-panel screwed joints used in the three-storey CLT building, including half-lap and spline joints in the wall-to-wall and wall-to-floor panel connections in shear and axial directions.

The individual isolated tests in axial and shear directions followed the standard procedure for cyclic joint testing with mechanical fasteners as prescribed by EN12512 (CEN, 2005). The provided test results have been used in this paper for calibrating unidirectional nonlinear springs in OpenSees (McKenna 2011). The *Pinching4* nonlinear spring has been utilised to model the behaviour of CLT connectors in this research. As depicted in Fig. 1, eight critical breakpoints, designated as ePd1, ePf1 through ePd4, ePf4 for the positive segments, and eNd1, eNf1 through eNd4, eNf4 for the negative segments, constitute the foundational structure of the spring. Furthermore, the unload-reload branches are regulated by six additional points, which can be used for matching the envelope curve with the connectors’ experimental behaviour. Since the area under each cycle of Force–Displacement hysteretic curve represents the energy absorbed per loading cycle, it is essential to consider the strength and stiffness degradation in the connectors’ behaviour, which affects the area under the curve. For this purpose, the model utilises fifteen parameters to control stiffness and strength degradation during cyclic loading, as mentioned in Fig. 1.

Figure 2 illustrates the calibration of angle bracket behaviour in the shear and tension directions. The ability to control the unload-reload branches, stiffness, and strength degradation of the applied nonlinear spring provides a close prediction of energy absorption. The *Pinching4* spring accounts for the pinching effect resulting from irreversible damage of wood crushing in the vicinity of the fasteners, which deteriorates the connectors’ stiffness under cyclic and seismic loads (Chan et al. 2023). This effect gradually reduces the connectors’ strength and energy absorption capacity, playing a vital role in the seismic performance of CLT buildings. The mechanical properties of the connectors, including their elastic and plastic stiffness, maximum stress and displacement, and strength degradation, have been considered to calibrate the connectors’ behaviour in both shear and axial directions. Figure 2(a) and 1(b) depict the angle bracket tests in shear and axial directions, respectively. The numerical results are compared with the experimental results in Fig. 2(c) for shear and 1(d) for axial directions.

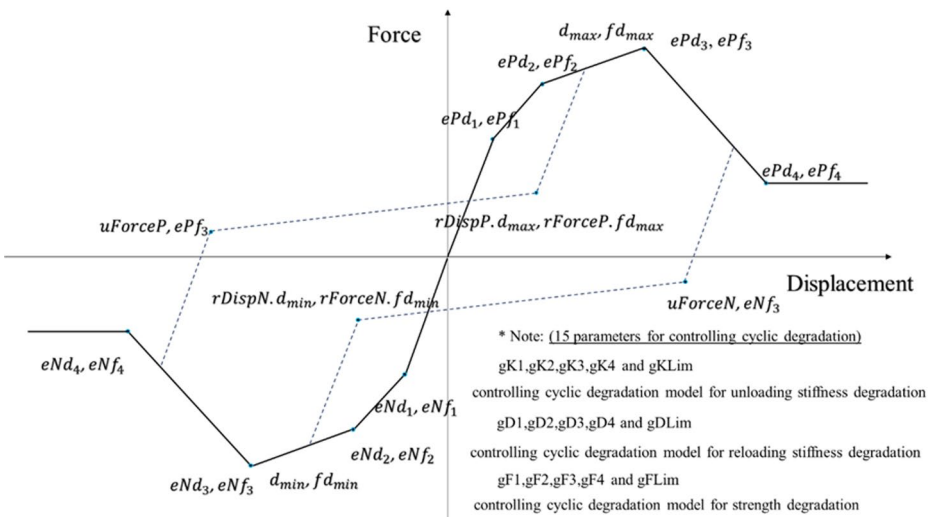


Fig. 1 *Pinching4* nonlinear spring backbone curve

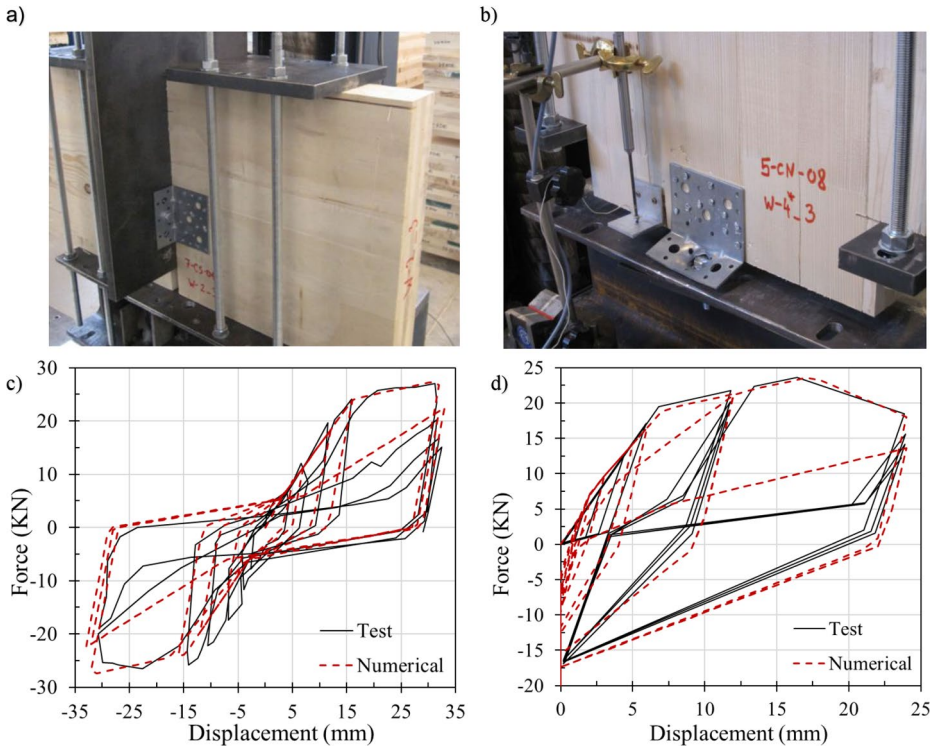


Fig. 2 Angle bracket test loaded in **a)** shear, **b)** tension (Gavric et al. 2015c), and experimental and numerical comparison in **c)** shear and **d)** tension directions

2.2 Wall level

The rigidity of screwed joints in coupled CLT wall systems affects their structural performance. When the joints are rigid, they increase the overall stiffness and strength of the wall system, causing it to behave similarly to a monolithic panel. Conversely, less rigid joints allow for relative movement between panels, which decreases stiffness but improves the system's deformation capacity (Gavric et al. 2015a). Figure 3(a) illustrates the studied coupled CLT shear wall configuration. Analytical analysis of single and coupled CLT shear walls without openings has confirmed that the overall behaviour of CLT shear walls mostly depends on rocking and sliding, as the in-plane deformations of the panels (shear and bending) are negligible (Gavric et al. 2015a; Popovski and Gavric 2016). Accordingly, CLT panels have been modelled using linear beam elements connected using moment-resisting connections with high stiffness ($E = 10^4$ GPa), acting as rigid frames as shown in Fig. 3(b). The *Pinching4* springs and linear beam elements have been employed to simulate the behaviour of the coupled shear wall (Wall II.4) tested by (Gavric et al. 2015a).

Gavric et al. (2015a) tested single and coupled CLT shear walls subjected to a constant axial load and reversed cyclic displacement. Wall II.4 has been modelled in this paper, which consisted of two panels connected via five screwed joints, with each panel anchored to the rigid base using two hold-downs at the corners and two angle brackets in the middle

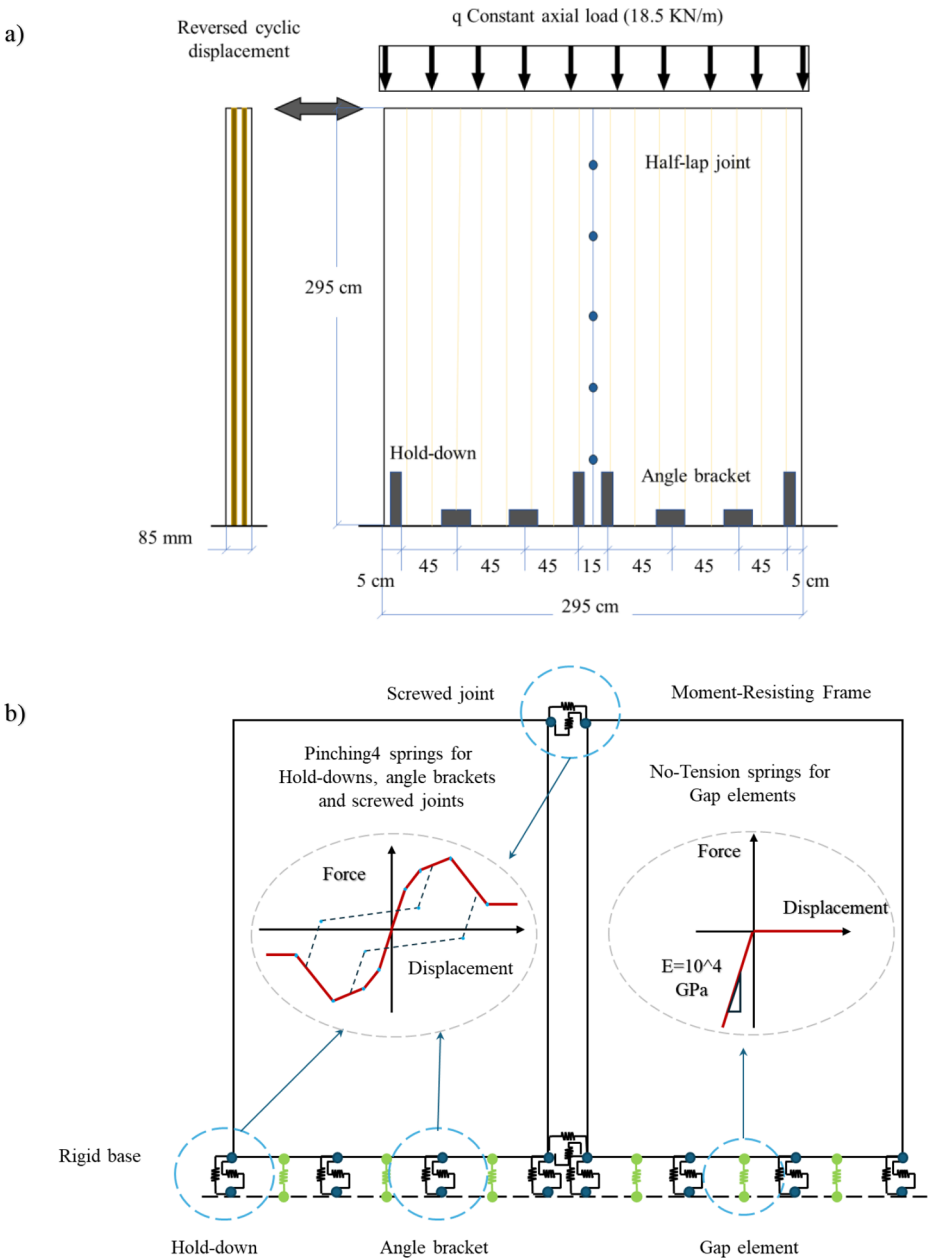


Fig. 3 a) Tested wall configuration and b) numerical modelling approach

of each wall segment, as shown in Fig. 3(a). The behaviours of the angle brackets and hold-downs are modelled using two non-linear springs representing the axial and shear behaviours. Screwed joints have parallel behaviours, so their shear behaviour is represented by the combined action of two springs connecting the panels. Gap joints only transfer compression

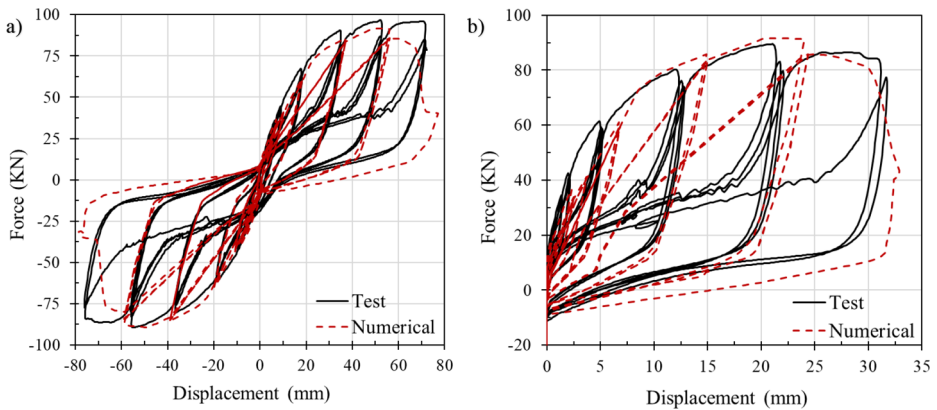


Fig. 4 Test and numerical comparison of the shear wall subjected to reversed cyclic load **a)** overall behaviour and **b)** uplift

Table 1 Test and numerical comparison of the overall behaviour of the modelled CLT shear wall

Parameter	Test <i>P</i>	Test <i>N</i>	Num <i>P</i>	Num <i>N</i>	Error <i>P</i> (%)	Error <i>N</i> (%)
Stiffness (kN/mm)	4.76	4.04	4.6	4.0	3.36	1
Yield point (kN)	73.83	64.64	74.35	71.32	0.7	10.3
Maximum strength (kN)	96.66	89.48	91.6	89.28	5.2	0.22

*Positive (*P*), Negative (*N*)

forces between panels and the rigid foundation without the ability to carry tensile forces. Hence, a high stiffness ($E_{\text{Gap}}=10^4$ GPa) has been assigned to the compression part of the gap element. The CLT panels have been observed to have rigid behaviour and insignificant shear and bending deformations compared to the connectors (Popovski and Gavric 2016).

Figure 4 depicts a graphical representation of the wall's response, illustrating the displacement of the upper corner of the wall versus the laterally applied force, and a detailed comparison of the experimental and numerical elastic stiffness, yield point and maximum strength is presented in Table 1. The lateral displacement of the top corner is the sum of the rocking and sliding of the panels, as shown in Fig. 4(a), disregarding in-plane shear and bending deformations. As the shear wall's overall behaviour results from the uplift and sliding, the test and numerical uplifts have been compared to confirm the right uplift-sliding combination. Figure 4(b) depicted the uplift at the bottom left corner of the wall.

2.3 Building level

The three-story building of the SOFIE project was tested on the unidirectional National Institute for Earth Science and Disaster Prevention (NIED) Shaking Table facility in Tsukuba, Japan, in July 2006 (Ceccotti 2008). This testing was part of a collaborative effort involving researchers from the Italian National Research Council – Threes and Timber Institute (CNR-IVALSA) and Japan (NIED). The project coordinated by CNR-IVALSA, aimed to explore the seismic and fire behaviour of multi-story CLT buildings. Configurations A and B had symmetric openings on the ground floor with various sizes, while the openings of configuration C were asymmetric. As presented in Fig. 5, the building had dimensions



Fig. 5 a) The three-story building of the SOFIE project configuration C b) first floor plan, c) south wall elevation (units in meters) (Ceccotti 2008)

of 7 m by 7 m and a height of 10 m with 4- and 2.3-meter-wide openings on the south and north ground floor walls, respectively. The walls were constructed with a thickness of 85 millimetres, comprising five layers of equal thickness, following the guidelines outlined in the EN C24 Timber class (Follesa et al. 2013).

Timber structures do not have a precise yielding point which makes the ductility definition difficult in most cases (Jorissen and Fragiaco 2011). In this case, the building has been designed for q-factor 1 according to the relevant design codes EC 8 and 5, and the design PGA prescribed by the code (PGAu, code), i.e. 0,35 g for the highest seismic zones in Italy (Ceccotti 2008). In this paper, Configuration C of the three-story building has been modelled in OpenSees. Moments resisting frames are employed to simulate the rigid behaviour of the CLT panels. The frames are connected to the foundation by *Pinching4* springs representing the angle brackets, hold-downs, and various types of screw joints as shown in Fig. 6. Gap elements are employed to transfer compressive forces at interfaces where panels

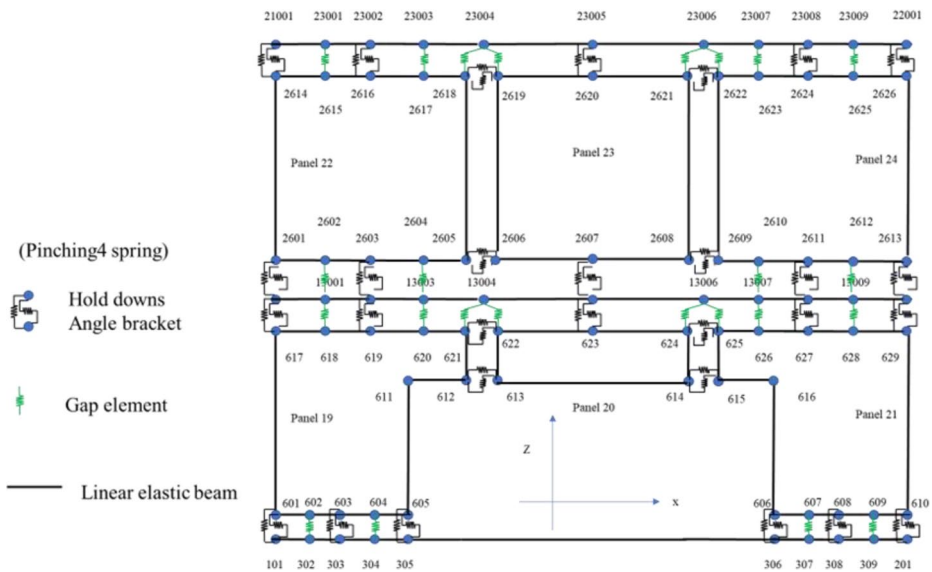


Fig. 6 FE modelling description of the ground and first floor of the CLT building (south side)

are in contact with each other or with the foundation in the absence of mechanical timber connections.

It has been observed that the wood-to-wood friction plays a crucial role in the CLT buildings' response and has been taken into account in advanced dynamic simulations. Comparing the test and numerical of the top displacement in the three-story building configuration B has shown that ignoring the friction effects results in a more flexible response. According to (Rinaldin and Fragiaco 2016), disregarding friction resulted in overestimations of 40% for the maximum roof displacement and 23.7% for the first vibration period in this specific building setup. They utilised the *Wood-Spring* and applied the dynamic friction coefficient $\mu=0.6$ for the simulation of the three- and seven-story buildings of the SOFIE project (Rinaldin and Fragiaco 2016). The *Wood-spring* has been specifically developed for modelling the nonlinear behaviour of CLT connectors which considers strength degradation and friction effect.

Unlike the *Wood-Spring*, the *Pinching4* cannot consider the friction effect between the panels. Therefore, the panel-to-panel friction effect has been considered by increasing the initial stiffness of the *Pinching4* nonlinear springs. This adjustment increases the energy absorption ability of the connectors without using additional springs to consider the friction effect. The percentage increase in the connectors' initial stiffness is obtained by monitoring and matching all floors' corners displacements and ground floor uplifts of the building subjected to the *Kobe JMA* ground motion with $PGA=0.82\text{ g}$ during the full-scale model calibration process. Specifically, the initial shear stiffness of the angle brackets on the ground floor has been enhanced by 90%. Furthermore, the initial axial stiffness of both angle brackets and hold-downs on other floors has been improved by 40%. Each spring has three degrees of freedom characterized by its type and position. All springs have two in-plane behaviours in axial and shear directions and one linear elastic behaviour perpendicular to

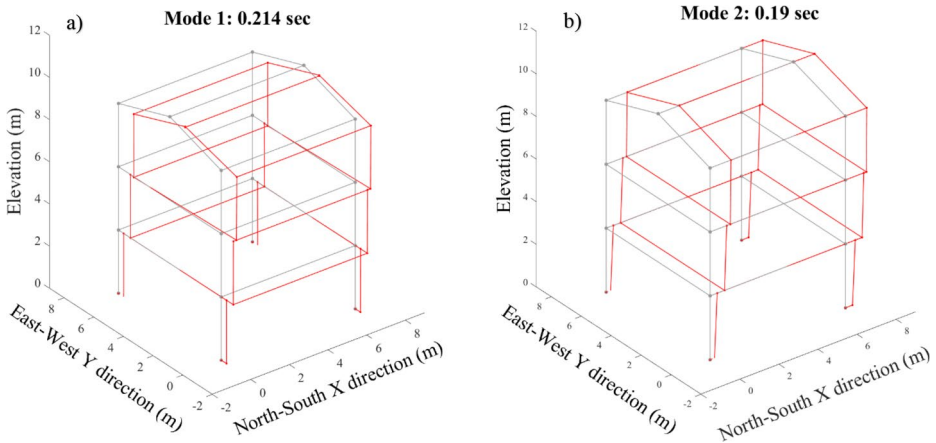


Fig. 7 a) First and b) second vibration mode shapes of the three-story building

Table 2 Test and numerical comparison of the fundamental periods, maximum displacements of the floor corners and uplift of the East side hold-downs on the ground floor of the Building

	Period (s)	Max. Displacement (mm)						Max. Uplift (mm)	
		1NE	1SE	2NE	2SE	3NE	3SE	0NE	0SE
Test	0.21	26	29.5	51.5	56.1	58.9	62.2	10.6	7.3
Model	0.214	32.2	33.4	49.2	50.7	59.7	61.1	10.9	6.8
Error	0.0	6.2	3.9	2.2	5.3	0.8	1.1	0.3	0.5
Error (%)	1.9%	23.9%	13.2%	4.4%	9.5%	1.3%	1.7%	3.0%	7.4%

the plane in the third direction. The out-of-plane behaviours have been considered elastic, with the same shear stiffness as the in-plane stiffness for all angle brackets and hold-downs.

The panel-to-panel friction effect is often overlooked in most simulations; however, this study considers the friction effect by increasing the initial stiffness of the connectors. This approach has certain limitations. Specifically, the calibration of friction is model-dependent, necessitating individual calibrations for each model. Additionally, the length of the panel-to-panel contact must be taken into account, particularly when large openings, such as doors, are present in the panels.

During the shaking table test procedure, configuration C of the three-story building was subjected to unidirectional Kobe JMA ground motion with PGA=0.82 g in the north-east direction (Ceccotti 2008). The natural vibration period was recorded as 0.21 s. The maximum displacements of the east side corners of the floors and uplifts recorded from the test have been utilised for numerical modelling validation. Figure 7 illustrates the first and second natural vibration modal shapes of the building.

The comparison between the experimental and numerical first vibration period of the building showed a highly accurate match with a 1.9% difference. Table 2 illustrates the maximum displacements of the floor corners and the uplifts at the ground floor corners as observed in the test and predicted by the model. In Table 2, the abbreviations NE and SE denote the North-East and South-East corners, respectively. The numerical values represent the floors within the building, where 0 corresponds to the ground floor, and 3 refers to the

roof floor. The predicted maximum displacements of the north and south corners of the third floor on the east side are 1.3 and 1.7% lower than those observed in the test. Additionally, the base corner uplifts differ by 3 and 7.5% compared to the test, respectively, at the North-East and South-East sides of the building.

3 Performance levels

According to (Rinaldi et al. 2023), the Significant Damage (SD) and Near Collapse (NC) limit states can be defined for dissipative connections in nonlinear analysis. The SD limit indicates the building is significantly damaged; however, it remains capable of carrying the vertical load. These states have been applied as damage indicators for connectors and then developed for the three-story CLT building (Rinaldi et al. 2023). These displacement-based limit states rely on the yield (δ_y) and ultimate (δ_u) displacements derived from the approximate trilinear load-displacement curve obtained from the first-cycle envelope, as depicted in the following equations:

$$\delta_{SD} = \frac{1}{\gamma_{RD,SD}} (\delta_y + 0.5(\delta_u - \delta_y)) \quad (1)$$

$$\delta_{NC} = \frac{\delta_U}{\gamma_{RD,NC}} \quad (2)$$

The partial factors on resistance for nonlinear analyses at the SD and NC limit states denoted as $\gamma_{RD,SD}$ and $\gamma_{RD,NC}$, are assumed to be 1 as it is prescribed for dissipative connections in the new Part 1–2 of EC 8. The model derives an approximate trilinear load-deformation curve from the initial cycle's envelope curve by connecting the points of yield load (Y), maximum load (M), and ultimate load (U) as illustrated in Fig. 8(a). According to EN 12,512, the yield load point (Y) is identified where the elastic line intersects the first cyclic envelope curve, which is shown in Fig. 8(b). This elastic line is plotted by linking points representing 10% and 40% of the maximum load on the initial cyclic envelope curve. The tangent at this intersection has a slope that is 1/6 of the elastic line's slope, as illustrated in Fig. 8(b) (Rinaldi et al. 2023). Using this method, the limit states for all connectors have

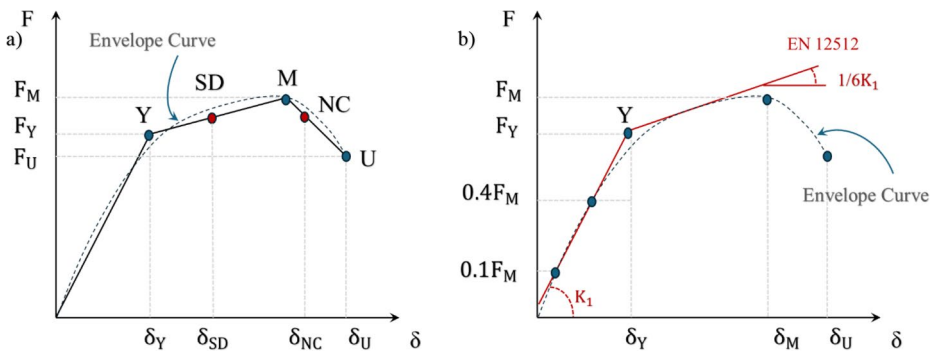


Fig. 8 a) Dissipative connections' SD and NC limit states on the trilinear load-deformation curve considering the first cycle envelope curve b) yield point determination based on EN12512 (CEN, 2005)

been precisely determined, subsequently establishing the building's limit states based on its connectors.

3.1 Modal push-over analysis (MPA)

To assess the building's performance while considering the effect of the fundamental mode, the Modal Push-over Analysis (MPA) has been conducted on the model (Gao et al. 2023). The forces have been applied to the mass centroid of each floor based on the first vibration mode of the building, as shown in Fig. 9(a). The base shear versus the ground-floor inter-story drift ratio graph for the three-story building of the SOFIE project in the East-West direction is depicted in Fig. 9(b). The ground-floor inter-story has been chosen as it experiences the largest inter-story drift among all floors. The SD and NC limit state inter-story drift ratios correspond to the point at which the first connector exceeds the limits. As depicted, the structural damage SD state occurred at the drift ratio of 0.0125, while the NC state was observed at 0.0195. The limit states for the three-story building have been presented in Fig. 9(b).

4 Fragility assessment

Several researchers have conducted experiments and computational analyses on CLT assemblies and structures to examine their performance under different static and dynamic loads (Fragiacomo et al. 2011; Latour and Rizzano 2017; Pozza et al. 2018c). (Ceccotti et al. 2006), (Ceccotti et al. 2010a), (Ceccotti et al. 2010b), (Dujic et al. 2010), (Ceccotti et al. 2013), (Follesa et al. 2013) and (Rinaldin and Fragiaco 2016) have developed models for SOFIE buildings and investigated their response to seismic loads. Since the behaviour of these buildings is influenced by the characteristics of ground motion, such as magnitude, frequency, duration, and soil type, comprehensive seismic simulations are necessary. However, the developed models have not been utilised for simulating CLT buildings subjected

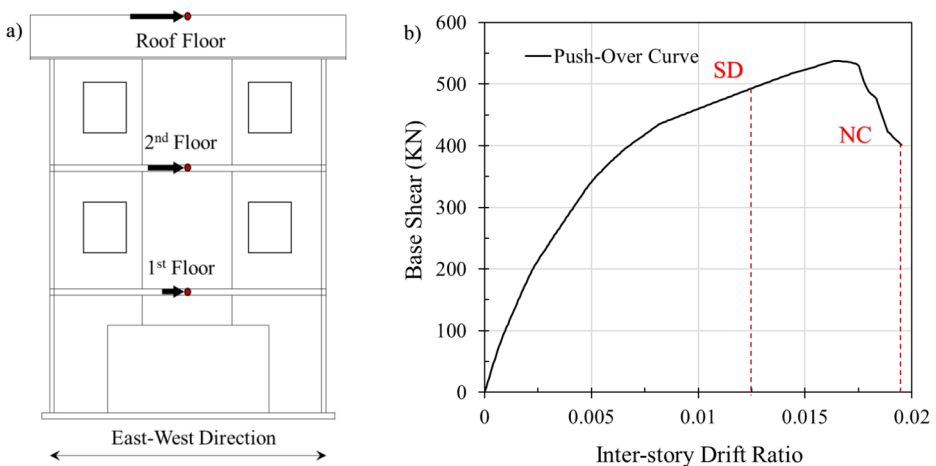


Fig. 9 a) Modal proportion displacements applied to the floors, and b) base shear versus the ground-floor inter-story drift ratio curve resulted from push-over analysis

to multiple ground motions, primarily due to the complexity and the time-consuming nature of such simulations. Additionally, this research considered various types of ground motion, an aspect not typically addressed in previous studies. To assess the demand and capacity accurately, nonlinear dynamic time-history analysis has been employed using a variety of ground motion records following the Quantification of Building Seismic Performance Factors (FEMA-P695) guidelines. FEMA-P695 has proposed the concept of IDA for evaluating the performance of structures subjected to seismic loads (FEMA 2009). The standardised records are specifically recommended for nonlinear dynamic analysis and collapse assessment. These records are structure-type and site hazard independent, cover a large number of events, consider Maximum Considered Earthquake (MCE) demands are sufficient for statistically robust evaluation of collapse capacity and are suitable for scaling in IDA.

This method relies on probabilistic seismic hazard analysis results to estimate a particular structure's seismic risk. This study exposed the validated numerical model to NF and FF ground motion records sets to assess the building's damage at SD and NC limit states. The NF set includes sites located within 10 km of the fault rupture, while the FF set includes sites beyond that distance. Within the NF record set, Pulse-like records (NF-P) have strong pulses in ground motion, while No Pulse records (NF-NP) lack such features, as detailed in Table 3. This set comprises 14 NF-P, 14 NF-NP, and 21 FF two-component records. The ground motions are independent of structural type and site-specific hazards, making them applicable to a wide range of structural systems and various site conditions (FEMA 2009).

Spectral acceleration at the building's fundamental period has been chosen as the Intensity Measure (IM). The geometric median of each two horizontal ground motion spectra has been employed to scale ground motions according to the first natural period of the three-story SOFIE building ($Sa(T1)$). The Sa has been scaled from 0.1 to 5 g at 0.1 intervals to simulate the increasing intensity of records. Consequently, the building has undergone analysis 50 times for each bidirectional ground motion in OpenSees, resulting in a 2450 time history analysis. The building performance has been evaluated based on each analysis's maximum recorded inter-story drift ratio. Figure 10 illustrates the building's maximum inter-story drift versus spectral acceleration at the building's first natural period under the NF-P and NF-NP record sets. Dashed lines show the 16 and 84 percentile deviations from the median value of the building response, demonstrating the upper and lower bounds in each graphical presentation.

The building's response subjected to the NF-P and NF-NP ground motions has been presented in Fig. 10(a and b), while Fig. 10(c) shows both NF-P and NF-NP. Notably, the building response subjected to NF-P ground motions has a broader bound compared to the NF-NP set, and the median value of the building collapse capacity under NF-P is observed to be 17.2% lower than NF-NP ground motions. Figure 10(d) presents the building's response under FF ground motions. The comparative graph presented in Fig. 10(f) reveals that the building collapse capacity under FF is higher than NF ground motions by 10.3%. This confirms that the NF-P ground motions trigger higher damage to the building due to the presence of stronger pulses compared to NF-NP. Furthermore, NF ground motions have a greater impact on the building and cause more severe damage than FF ground motions. Accordingly, the building has shown a lower collapse capacity subjected to the NF compared to FF ground motions, confirming the impact of the distance of the building and fault rupture.

Table 3 NF and FF ground motion details (FEMA 2009)

No	Record set	PEER-NGA Number	Year	Event	Station
1	NF-P	181	1979	Imperial Valley-06	El Centro Array #6
2	NF-P	182	1979	Imperial Valley-06	El Centro Array #7
3	NF-P	292	1980	Irpinia, Italy-01	Sturno
4	NF-P	723	1987	Superstition Hills-02	Parachute Test Site
5	NF-P	802	1989	Loma Prieta	Saratoga - Aloha Ave
6	NF-P	821	1992	Erzican, Turkey	Erzincan
7	NF-P	828	1992	Cape Mendocino	Petrolia
8	NF-P	879	1992	Landers	Lucerne
9	NF-P	1063	1994	Northridge-01	Rinaldi Receiving Sta
10	NF-P	1086	1994	Northridge-01	Sylmar - Olive View Med FF
11	NF-P	1165	1999	Kocaeli, Turkey	Izmit
12	NF-P	1503	1999	Chi-Chi, Taiwan	TCU065
13	NF-P	1529	1999	Chi-Chi, Taiwan	TCU102
14	NF-P	1605	1999	Duzce, Turkey	Duzce
15	NF-NP	126	1976	Gazli, USSR	Karakyr
16	NF-NP	160	1979	Imperial Valley-06	Bonds Corner
17	NF-NP	165	1979	Imperial Valley-06	Chihuahua
18	NF-NP	495	1985	Nahanni, Canada	Site 1
19	NF-NP	496	1985	Nahanni, Canada	Site 2
20	NF-NP	741	1989	Loma Prieta	BRAN
21	NF-NP	753	1989	Loma Prieta	Corralitos
22	NF-NP	825	1992	Cape Mendocino	Cape Mendocino
23	NF-NP	1004	1994	Northridge-01	LA - Sepulveda VA Hospital
24	NF-NP	1048	1994	Northridge-01	Northridge - 17,645 Saticoy St
25	NF-NP	1176	1999	Kocaeli, Turkey	Yarimca
26	NF-NP	1504	1999	Chi-Chi, Taiwan	TCU067
27	NF-NP	1517	1999	Chi-Chi, Taiwan	TCU084
28	NF-NP	2114	2002	Denali, Alaska	TAPS Pump Station #10
29	FF	953	1994	Northridge	Beverly Hills - Mulhol
30	FF	960	1994	Northridge	Canyon Country-WLC
31	FF	1602	1999	Duzce, Turkey	Bolu
32	FF	1787	1999	Hector Mine	Hector
33	FF	169	1979	Imperial Valley	Delta
34	FF	174	1979	Imperial Valley	El Centro Array #11
35	FF	1111	1995	Kobe, Japan	Nishi-Akashi
36	FF	1116	1995	Kobe, Japan	Shin-Osaka
37	FF	1158	1999	Kocaeli, Turkey	Duzce
38	FF	1148	1999	Kocaeli, Turkey	Arcelik
39	FF	900	1992	Landers	Yermo Fire Station
40	FF	848	1992	Landers	Coolwater
41	FF	752	1989	Loma Prieta	Capitola
42	FF	767	1989	Loma Prieta	Gilroy Array #3
43	FF	1633	1990	Manjil, Iran	Abbar
44	FF	721	1987	Superstition Hills	El Centro Imp. Co.
45	FF	725	1987	Superstition Hills	Poe Road (temp)
46	FF	1244	1999	Chi-Chi, Taiwan	CHY101
47	FF	1485	1999	Chi-Chi, Taiwan	TCU045
48	FF	68	1971	San Fernando	LA - Hollywood Stor
49	FF	125	1976	Friuli, Italy	Tolmezzo

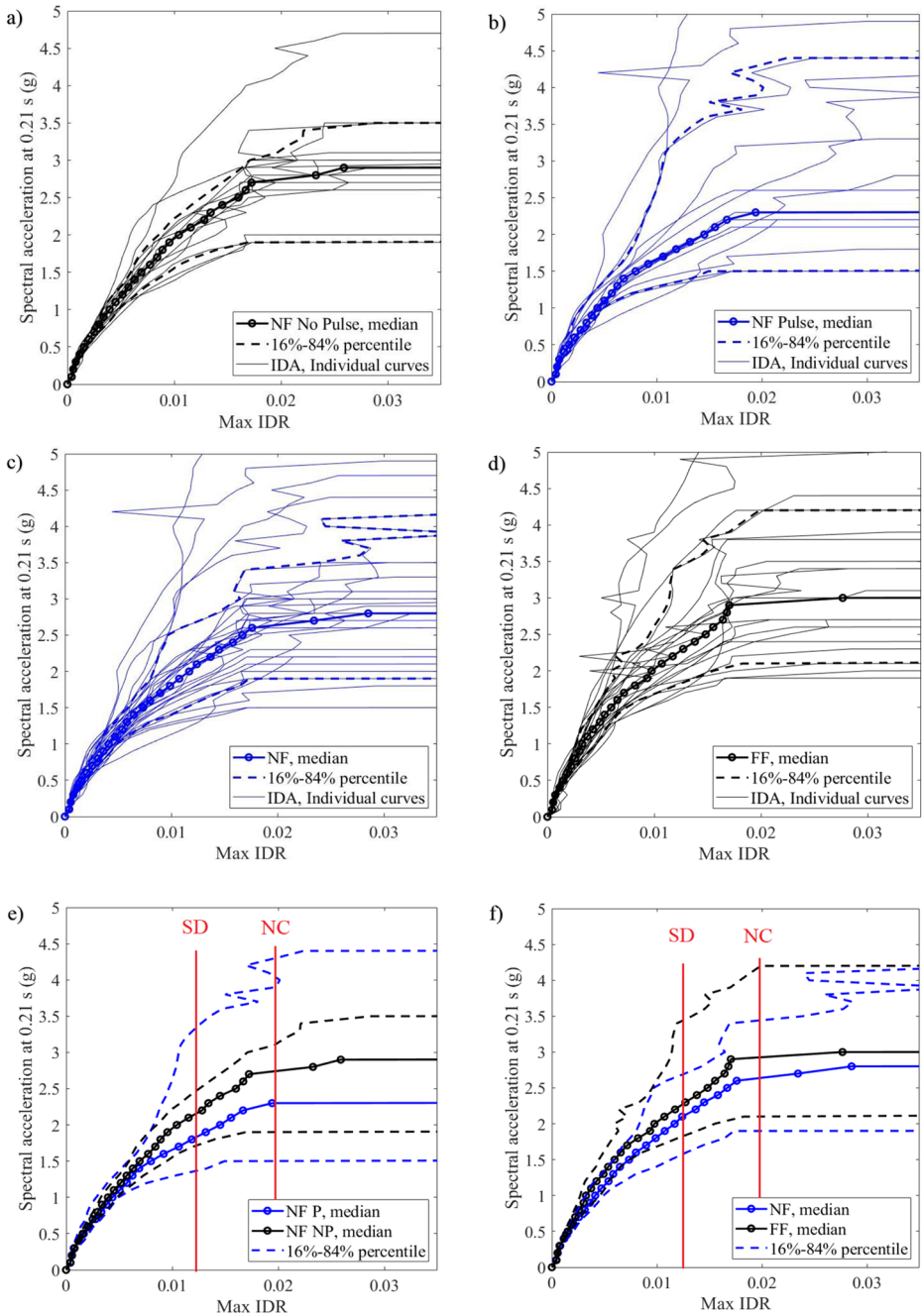


Fig. 10 IDA curves for the building subjected to the (a) NF No-pulse, (b) NF Pulse, (c) NF Pulse and No pulse, (d) FF (e) NF Pulse and No-pulse median, (f) NF and FF median ground motions

4.1 Fragility assessment

Fragility curves quantify the damage states of buildings under varying levels of seismic hazards. By associating these damage states with specific hazard levels, fragility curves enable the prediction of potential losses (Cornell 1968). (Tefamariam et al. 2014) examined the seismic vulnerability of hybrid steel-timber structures with CLT infills, indicating the potential of varying CLT configurations to achieve diverse performance objectives in earthquake engineering. Similarly, (Teweldebrhan et al. 2023) studied the CLT-coupled wall systems for improving seismic resilience, utilising a bi-variate probabilistic seismic fragility assessment. (Aloisio et al. 2021) assessed the fragility functions and behaviour factors of multi-story CLT structures characterized by the energy-dependent generalized Bouc-Wen hysteresis model. By applying the IDA of buildings, they investigated the impact of the number of stories and CLT panel configurations on the seismic performance of the models. This study derives the fragility curves for the three-story building of the SOFIE project, utilising IDA simulations. These simulations are based on statistical analyses of the building’s response when subjected to NF and FF ground motions.

For each damage state, IDA results have been statistically analysed and the lognormal distribution parameters have been found. The cumulative distribution function (CDF) of the lognormal distribution is defined as follows:

$$P(C|IM = x) = \Phi \left(\frac{\ln(x) - \ln(\theta)}{\beta} \right) \tag{3}$$

Where, $P(C|IM=x)$ represents the collapse probability of a structure subjected to ground motion with an IM of x , calculated using the standard normal cumulative distribution function (Φ). The fragility function’s median (θ) and logarithmic standard deviation (β) are calculated using the moment estimator method, which is well-suited for IDA.

$$\ln(\theta) = \frac{1}{n} \sum_{i=1}^n \ln IM_i \tag{4}$$

$$\beta = \sqrt{\frac{1}{n-1} \sum_{i=1}^n \left(\ln IM_i - \ln(\hat{\theta}) \right)^2} \tag{5}$$

n represents the total number of ground motions examined, with IM_i denoting the IM value corresponding to the initial collapse condition for the i^{th} ground motion. Given the lognormal distribution of IM, the mean and median of $\ln(IM)$ are equivalent. Fragility curves for the three-story building subjected to NF and FF ground motions are presented in Fig. 11. Specifically, the building’s fragility curves for NF, including both pulse and no-pulse types, and for FF ground motion sets are depicted in Fig. 11(a and b), respectively. These graphs illustrate the building’s susceptibility to SD and NC as a function of the building’s spectral acceleration in the first period. The building is more vulnerable to NF ground motions. For instance, at $Sa(T1)=1.5$ g, there is a 45% probability of exceedance of SD and a 25% probability of exceedance of NC damage, while when exposed to FF ground motions, the probability of exceedance of SD and NC are 35% and 20%, respectively.

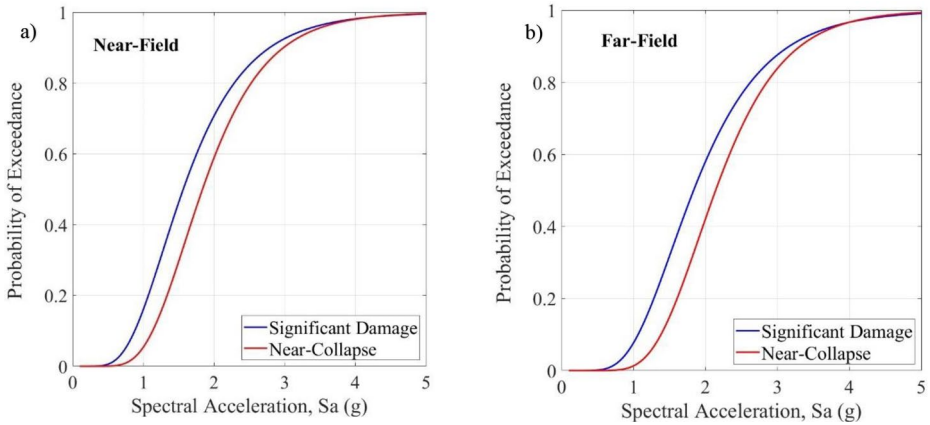


Fig. 11 Fragility curves for building under a) NF and b) FF ground motions

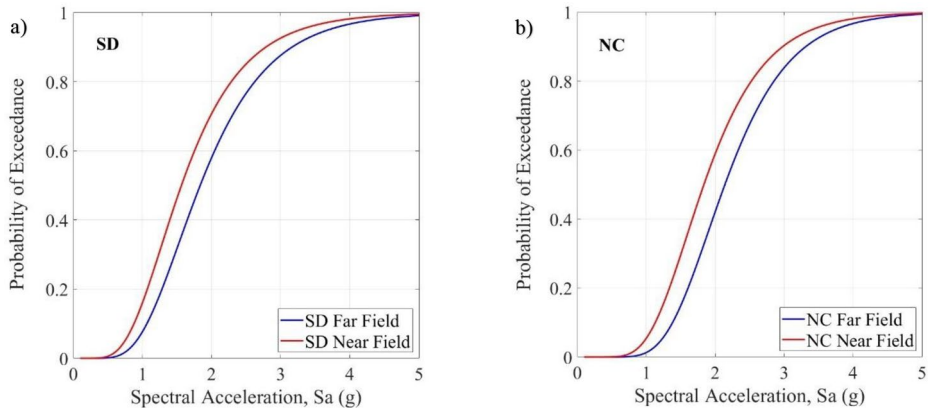


Fig. 12 Fragility curves for building under FF and NF ground motions a) SD and b) NC limit states

Figure 12 shows a comparison of the fragility curves for SD and NC damage states under both NF and FF ground motions. When the building is subjected to NF ground motions at $Sa(T1)=1.5$ g, there is a 45% probability of exceedance of SD, while it drops to 35% under FF ground motions. Similarly, for the NC limit state, the building has a 25% probability of exceedance of reaching NC under NF ground motions, compared to a 20% probability when subjected to FF ground motions at a spectral acceleration of 1.5 g. The results indicate the distinctive impact of the ground motion characteristics on the CLT building’s seismic response. Therefore, NF ground motions have a more severe impact on CLT buildings considered in this paper compared to FF due to the proximity to earthquake fault ruptures and the occurrence of pulse-like ground motions. The results show a clear impact of ground motion characteristics on the seismic response of the building. The severe nature of NF ground motions on these buildings is well recognized. Therefore, studying specific vulnerabilities related to connector performance in these structures is important. Under NF conditions, bursts of energy can cause significant deformation of connectors and may lead

to screws being pulled out. This presents a problem considering the complex load paths in CLT structures. The intense shocks and pulse-like motions typical of NF scenarios place extraordinary demands on the structural integrity and present challenges for connectors that are not easily replaceable.

The more severe impact of NF ground motions, particularly NF-P records, has resulted in higher probabilities of SD and NC. This increased vulnerability is primarily due to the distinct characteristics of NF motions, including shorter distance from the seismic source, large velocity pulses, high energy content over short durations, and directivity effects caused by rupture propagation toward the site. These features lead to abrupt and concentrated energy input, placing more severe and sudden demands on the structural system. In comparison, NF-NP motions within the NF category result in lower exceedance probabilities, especially for the NC limit state. FF ground motions, which originate at greater distances, tend to deliver energy more gradually, leading to reduced peak demands and, consequently, lower probabilities of SD and NC.

To mitigate the increased vulnerability associated with NF ground motions, particularly NF-P records, adopting energy dissipative devices can be explored in CLT and hybrid structural systems that integrate CLT with steel or concrete. These systems can improve buildings' overall performance, particularly in seismic regions. Self-centring connections have demonstrated significant potential in dissipating seismic energy while minimising residual displacement through controlled slippage mechanisms, utilizing post-tensioning and friction-based techniques. By reducing damage accumulation and facilitating faster post-event recovery, these advanced connections can substantially improve the safety and serviceability of CLT structures.

5 Conclusion

This research investigates the seismic vulnerability of the three-story CLT building of the SOFIE project using IDA, focusing on its response to NF and FF ground motions proposed by FEMA P-965. To achieve this, finite element models have been developed at the component, wall, and full-building scales in OpenSees and have been validated against experimental results. The study shows significant differences in the CLT building's response to NF-P and NF-NP ground motions. Notably, the NF-P ground motions induce a broader range of the CLT building responses and a substantially lower median collapse capacity compared to NF-NP, indicating a higher vulnerability to pulse-like seismic activities characteristic of NF ground motions. The IDA curves prove that the CLT building considered in this paper is more affected by NF-P than by NF-NP and FF ground motions. Specifically, the collapse capacity is 17.2% lower subjected to NF-P comparing NF-NP. This difference results in higher damage potential from NF-P due to stronger seismic pulses. Additionally, the studied CLT building shows a 10.3% higher collapse capacity under FF than NF ground motions. This suggests that the CLT building's proximity to the seismic fault significantly influences its vulnerability to collapse, with NF ground motions causing more damage than FF.

The fragility curves were derived to assess the seismic vulnerability of the CLT building, confirming the importance of associating damage states with specific seismic hazard levels for accurate prediction of potential losses. The fragility analysis demonstrates that the studied building is more vulnerable when subjected to NF ground motions than to FF. For

instance, at a spectral acceleration of $S_a(T_1)=1.5$ g, there is a 45% probability of exceedance of SD, whereas this probability decreases to 35% under FF ground motions. Similarly, for the NC damage state, the considered CLT building in this study has a 25% probability of exceedance of reaching NC under NF ground motions, in contrast to a 20% probability of exceedance under FF ground motions.

The findings demonstrate that the considered CLT building in this study is more severely impacted by NF ground motions due to their closer proximity to earthquake faults and the sudden, intense shocks characteristic of these motions. Such ground motions place greater demands on structures, especially those sensitive to these pulse-like responses, resulting in significantly more damage than FF ground motions. The characteristics of ground motion should be considered in the design of CLT buildings to mitigate the risk of damage and improve their safety in seismic events. Future studies should investigate the optimization of structural design, and the impact of large openings on panel performance to improve safety and reduce the collapse potential of CLT buildings.

Author contributions Saeid Javidi and Mohammad Reza Salami contributed to the study conception and design, data collection, modelling, and analysis. Igor Gavric' participated in providing data and validation. The first draft of the manuscript was written by Saeid Javidi, and Mohammad Reza Salami, Igor Gavric', and Georgios Fourlaris reviewed and provided feedback on the manuscript. All authors read and approved the final manuscript.

Funding The authors declare that no funds, grants, or other support were received during the preparation of this manuscript.

Data availability The datasets generated during and/or analysed during the current study are available from the corresponding author on reasonable request.

Declarations

Competing interests The authors have no relevant financial or non-financial interests to disclose.

Open Access This article is licensed under a Creative Commons Attribution 4.0 International License, which permits use, sharing, adaptation, distribution and reproduction in any medium or format, as long as you give appropriate credit to the original author(s) and the source, provide a link to the Creative Commons licence, and indicate if changes were made. The images or other third party material in this article are included in the article's Creative Commons licence, unless indicated otherwise in a credit line to the material. If material is not included in the article's Creative Commons licence and your intended use is not permitted by statutory regulation or exceeds the permitted use, you will need to obtain permission directly from the copyright holder. To view a copy of this licence, visit <http://creativecommons.org/licenses/by/4.0/>.

References

- Aloisio A, Alaggio R, Fragiaco M (2021) Fragility functions and behavior factors Estimation of multi-story cross-laminated timber structures characterized by an energy-dependent hysteretic model. *Earthq Spectra* 37:134–159
- Aloisio A, Pellicciari M, Sirotti S, Boggian F, Tomasi R (2022) Optimization of the structural coupling between RC frames, CLT shear walls and asymmetric friction connections. *Bull Earthq Eng* 20:3775–3800
- Bezabeh MA, Tesfamariam S, Stiemer SF, Popovski M, Karacabeyli E (2016) Direct displacement-based design of a novel hybrid structure: steel moment-resisting frames with cross-laminated timber infill walls. *Earthq Spectra* 32:1565–1585
- Bezabeh M, Bitsuamlak G, Tesfamariam S (2018) Risk-based wind design of tall mass-timber buildings. *The*

- Casagrande D, Doudak G, Polastri A (2019) A proposal for the capacity-design at wall-and building-level in light-frame and cross-laminated timber buildings. *Bull Earthq Eng* 17:3139–3167
- Ceccotti A (2008) New technologies for construction of medium-rise buildings in seismic regions: the XLAM case. *Struct Eng Int* 18:156–165
- Ceccotti A, Follesa M, Lauriola MP, Sandhaas C, Minowa C, Kawai N, Yasumura M (2006) Which seismic behaviour factor for multi-storey buildings made of cross-laminated wooden panels. Proceedings of 39th CIB W18 Meeting, paper, 4
- Ceccotti A, Sandhaas C, Yasumura M (2010a) Seismic behaviour of multistorey cross-laminated timber buildings. Proceedings of the International Convention of Society of Wood Science and Technology and United Nations Economic Commission for Europe-Timber Committee, 1–14
- Ceccotti A, Sandhaas C, Yasumura M (2010b) Seismic performance of X-Lam buildings: the Italian SOFIE project. 9th US National and 10th Canadian Conference on Earthquake Engineering, Toronto, Canada
- Ceccotti A, Sandhaas C, Okabe M, Yasumura M, Minowa C, Kawai N (2013) SOFIE project–3D shaking table test on a seven-storey full-scale cross-laminated timber Building. *Earthq Eng Struct Dynamics* 42:2003–2021
- Chan N, Hashemi A, Agarwal S, Zarnani P, Quenneville P (2023) Experimental testing of a rocking cross-laminated timber wall with pinching-free connectors. *J Struct Eng* 149:04023132
- Christovasilis I, Riparbelli L, Rinaldin G, Tamagnone G (2020) Methods for practice-oriented linear analysis in seismic design of cross laminated timber buildings. *Soil Dynamics Earthq Eng* 128:105869
- Code P (2005) Eurocode 8: design of structures for earthquake resistance-part 1: general rules, seismic actions and rules for buildings. European Committee for Standardization, Brussels
- Cornell CA (1968) Engineering seismic risk analysis. *Bull Seismol Soc Am* 58:1583–1606
- Dujic B, Strus K, Zarnic R, Ceccotti A (2010) Prediction of dynamic response of a 7-storey massive XLam wooden building tested on a shaking table. Proceedings of the 11th world conference on timber engineering WCTE, Riva del Garda, Italy
- European Committee for Standardization (2005) Timber structures test methods-Cyclic testing of joints made with mechanical fasteners. CEN Brussels, Belgium
- Fema P (2009) Quantification of building seismic performance factors. Washington, DC
- Follesa M, Fragiaco M (2018) Force-based seismic design of mixed CLT/Light-Frame buildings. *Eng Struct* 168:628–642
- Follesa M, Christovasilis IP, Vassallo D, Fragiaco M, Ceccotti A (2013) Seismic design of multi-storey cross laminated timber buildings according to Eurocode 8. *Ingegneria Sismica*, 4
- Fragiaco M, Dujic B, Sustersic I (2011) Elastic and ductile design of multi-storey crosslam massive wooden buildings under seismic actions. *Eng Struct* 33:3043–3053
- Gao Z, Zhao M, Du X (2023) Modal pushover analysis for seismic performance assessment of underground structures. *J Earthquake Eng* 27:1196–1214
- Gavric I, Popovski M (2014) Design models for CLT shearwalls and assemblies based on connection properties. Proceedings of the INTER Conference, Bath, UK, 1–4
- Gavric I, Fragiaco M, Ceccotti A (2015a) Cyclic behavior of CLT wall systems: experimental tests and analytical prediction models. *J Struct Eng* 141:04015034
- Gavric I, Fragiaco M, Ceccotti A (2015b) Cyclic behavior of typical screwed connections for cross-laminated (CLT) structures. *Eur J Wood Wood Product* 73:179–191
- Gavric I, Fragiaco M, Ceccotti A (2015c) Cyclic behaviour of typical metal connectors for cross-laminated (CLT) structures. *Mater Struct* 48:1841–1857
- Green M, Taggart J (2020) *Tall wood buildings: Design, construction and performance*, Birkhäuser
- Ho TX, Dao TN, Van De Lindt JW, Pryor S (2024) Performance-Based design of posttensioned Cross-Laminated timber and Light-Frame wood shear wall hybrid system. *J Struct Eng* 150:04024017
- Jorissen A, Fragiaco M (2011) General notes on ductility in timber structures. *Eng Struct* 33:2987–2997
- Kovacs MA, Wiebe L (2019) Controlled rocking CLT walls for buildings in regions of moderate seismicity: design procedure and numerical collapse assessment. *J Earthquake Eng* 23:750–770
- Latour M, Rizzano G (2017) Seismic behavior of cross-laminated timber panel buildings equipped with traditional and innovative connectors. *Archives Civil Mech Eng* 17:382–399
- Mckenna F (2011) OpenSees: a framework for earthquake engineering simulation. *Comput Sci Eng* 13:58–66
- Pan Y, Shahnewaz M, Tannert T (2023) Seismic performance and collapse fragility of balloon-framed CLT school Building. *J Earthquake Eng* 27:3115–3135
- Popovski M, Gavric I (2016) Performance of a 2-storey CLT house subjected to lateral loads. *J Struct Eng* 142:E4015006
- Popovski M, Gavric I, Schneider J (2014) Performance of two-storey CLT house subjected to lateral loads. Proceedings of the World Conference on Timber Engineering, Quebec City, QC, Canada
- Pozza L, Ferracuti B, Massari M, Savoia M (2018a) Axial–Shear interaction on CLT hold-down connections–Experimental investigation. *Eng Struct* 160:95–110

- Pozza L, Saetta A, Savoia M, Talledo D (2018b) Angle bracket connections for CLT structures: experimental characterization and numerical modelling. *Constr Build Mater* 191:95–113
- Pozza L, Savoia M, Franco L, Saetta A, Talledo D (2018c) Effect of different modelling approaches on the prediction of the seismic response of multi-storey CLT buildings. *Timber Struct Eng* 163
- Rinaldi V, Casagrande D, Fragiaco M (2023) Verification of the behaviour factors proposed in the second generation of eurocode 8 for cross-laminated timber buildings. *Earthq Eng Struct Dynamics* 52:910–931
- Rinaldin G, Fragiaco M (2016) Non-linear simulation of shaking-table tests on 3-and 7-storey X-Lam timber buildings. *Eng Struct* 113:133–148
- Roncari A, Gobbi F, Loss C (2020) Nonlinear static seismic response of a Building equipped with hybrid cross-laminated timber floor diaphragms and concentric X-braced steel frames. *Buildings* 11:9
- Shahnewaz M, Pan Y, Shahria Alam M, Tannert T (2020) Seismic fragility estimates for cross-laminated timber platform Building. *J Struct Eng* 146:04020256
- Stepinac M, Šušteršič I, Gavrić I, Rajčić V (2020) Seismic design of timber buildings: highlighted challenges and future trends. *Appl Sci* 10:1380
- Tannert T, Loss C (2022) Contemporary and novel hold-down solutions for mass timber shear walls. *Buildings* 12:202
- Tesfamariam S, Stiemer S, Dickof C, Bezabeh M (2014) Seismic vulnerability assessment of hybrid steel-timber structure: steel moment-resisting frames with CLT infill. *J Earthquake Eng* 18:929–944
- Teweldebrhan BT, Goda K, De Risi R, Tesfamariam S (2023) Multi-variate seismic fragility assessment of CLT coupled wall systems. *Earthq Spectra* 39:2100–2122
- Vassallo D, Follesa M, Fragiaco M (2018) Seismic design of a six-storey CLT Building in Italy. *Eng Struct* 175:322–338
- Zhang C, Loss C (2023) Evaluation of seismic fragilities of special concentrically braced frame hybrid buildings equipped with prefabricated cross-laminated timber-steel composite floor diaphragms. *Bull Earthq Eng* 21:6423–6452

Publisher's note Springer Nature remains neutral with regard to jurisdictional claims in published maps and institutional affiliations.